Transition from hemifusion to pore opening is rate limiting for vacuole membrane fusion

Christoph Reese and Andreas Mayer

Département de Biochimie, Université de Lausanne, 1066 Epalinges, Switzerland

Fusion pore opening and expansion are considered the most energy-demanding steps in viral fusion. Whether this also applies to soluble *N*-ethyl-maleimide sensitive fusion protein attachment protein receptor (SNARE)– and Rab-dependent fusion events has been unknown. We have addressed the problem by characterizing the effects of lysophosphatidylcholine (LPC) and other late-stage inhibitors on lipid mixing and pore opening during vacuole fusion. LPC inhibits fusion by inducing positive curvature in the bilayer and changing its biophysical properties. The LPC block reversibly prevented formation of the hemifusion intermediate that allows lipid, but not content, mixing. Transition from hemifusion to pore opening was sensitive to guanosine-5′-(γ-thio)triphosphate. It required the vacuolar adenosine triphosphatase V_0 sector and coincided with its transformation. Pore opening was rate limiting for the reaction. As with viral fusion, opening the fusion pore may be the most energy-demanding step for intracellular, SNARE-dependent fusion reactions, suggesting that fundamental aspects of lipid mixing and pore opening are related for both systems.

Introduction

Protein-mediated fusion reactions are sensitive to membrane lipid composition (Chernomordik and Kozlov, 2003). Lipids such as phosphoinositides control the activity and concentration of fusion proteins (Simonsen et al., 2001). Lipids also directly influence bilayer mixing via their biophysical properties, i.e., charge and conformation, which determine the spontaneous curvature of membranes (Chernomordik et al., 1997). A physical influence on the membrane may also form the basis for effects of phosphatidylethanolamine on p97/p47–mediated Golgi–liposome fusion (Pecheur et al., 2002) and of cholesterol and sphingolipids, which are required for fusion of Semliki forest virus (Ahn et al., 2002).

Lysophosphatidylcholines (LPCs) exhibit positive spontaneous curvature (Fuller and Rand, 2001). They inhibit fusion of protein-free bilayers (Chernomordik et al., 1995; Wu et al., 1996), viral fusion (Chernomordik et al., 1997; Melikyan et al., 2000), exocytosis (Vogel et al., 1993), and microsome fusion (Chernomordik et al., 1993). LPCs show increasing inhibitory potency with increasing hydrocarbon chain length (Chernomordik et al., 1997), and they show equivalent effects in different fusion systems using very different proteinaceous machines. Therefore, LPCs probably act via lipid conformation and membrane curvature rather than by direct influence on fusion-relevant proteins.

Consequently, a universal physical intermediate of all bilayer fusion reactions was postulated that should be independent of the protein machinery inducing fusion and cannot be overcome in the presence of LPC. This intermediate may be a fusion stalk (Chernomordik and Zimmerberg, 1995; Kozlovsky et al., 2002; Chernomordik and Kozlov, 2003). In a stalk, the outer leaflets of two fusing bilayers are merged, whereas the inner leaflets remain separated. The stalk is a structure of negative membrane curvature. It can expand into a hemifusion state in which lipids from the inner monolayers associate to produce a new bilayer, the hemifusion diaphragm. Hemifusion is detectable for viral fusion systems, particularly if the normal fusion pathway is disturbed (Kemble et al., 1994; Melikyan et al., 1995, 2005; Chernomordik et al., 1998; Munoz-Barroso et al., 1998). It can also be generated in the polyethylene glycol–, hypotonic stress–, and cation-induced fusion of liposomes (Chanturiya et al., 1997; Lee and Lentz, 1997; Meers et al., 2000). Also, SNARE-dependent fusion can generate hemifusion states. Depending on the conditions, these can be unproductive alternative outcomes or intermediates on the pathway to full fusion (Giraudo et al., 2005; Lu et al., 2005; Reese et al., 2005; Xu et al., 2005).

Homotypic fusion of yeast vacuoles is a model reaction of SNARE-dependent intracellular fusion for which a cell-free

Correspondence to Andreas Mayer: Andreas.Mayer@unil.ch

Abbreviations used in this paper: ALP, alkaline phosphatase; BAPTA, 1,2-bis-(o-aminophenoxy)-ethane-N,N,N′,N′-tetraacetic acid; GTPγS, guanosine-5′-(γ-thio)triphosphate; LPC, lysophosphatidylcholine; MED, myristoylated alanine-rich C kinase substrate effector domain peptide; Rh-PE, lissamine rhodamine B 1,2-dihexadecanoyl-sn-glycero-3-phosphoethanolamine.

The Journal of Cell Biology, Vol. 171, No. 6, December 19, 2005 981–990
http://www.jcb.org/cgi/doi/10.1083/jcb.200510018

fusion assay is available (Mayer, 2002; Wickner, 2002). Vacuole fusion proceeds in several steps and depends on numerous proteins. In brief, the following events are relevant to this study: priming is characterized by the ATP-dependent rearrangements of SNAREs, GTPases, and tethering factors and is a prerequisite for subsequent steps. cis-SNARE complexes are disassembled by the ATPase Sec18p/NSF and its cofactor Sec17p/α-SNAP, which is released from the vacuole (Mayer et al., 1996; Ungermann et al., 1998a). The second step, membrane attachment, requires the Rab-GTPase Ypt7p and leads to the formation of trans-SNARE complexes between the fusion partners (Mayer and Wickner, 1997; Ungermann et al., 1998b). Trans-SNARE pairing triggers a measurable release of calcium from the vacuole (Peters and Mayer, 1998; Merz and Wickner, 2004b). V_0, the membrane integral part of the vacuolar H^+-ATPase, is required to complete fusion (Peters et al., 2001; Bayer et al., 2003; Thorngren et al., 2004).

In this study, we have modulated bilayer conformation by LPC and explored the effects on the fusion pathway of yeast vacuoles. The assay of lipid perturbation promises important insights into the fusion mechanism, such as the timing of bilayer merger and factors required to induce it. We performed a kinetic analysis to map the LPC-sensitive step and correlated these data to molecular marker events for docking and postdocking events in order to determine the rate-limiting stage of vacuole fusion.

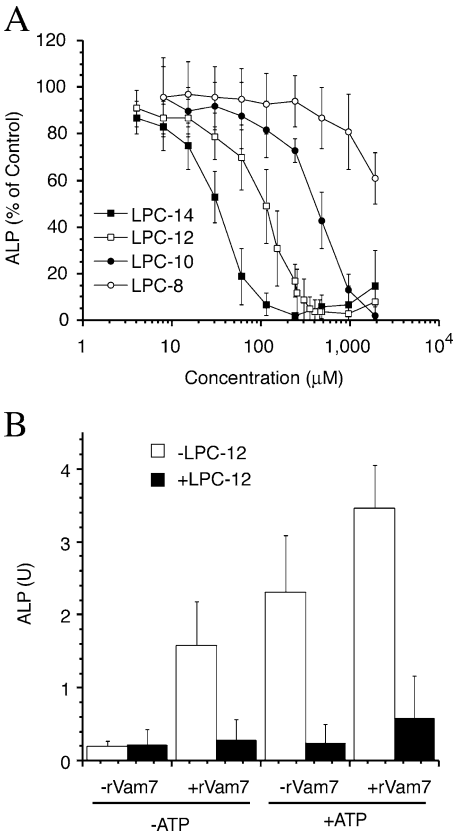

Figure 1. **LPC inhibits vacuole fusion.** (A) Titration of four different LPCs. Standard fusion reactions were incubated at 27°C in the presence of the indicated inhibitors at increasing concentrations. One sample was kept on ice. After 70 min, fusion activity was assayed. Values were normalized to the controls without inhibitors, and ice values were subtracted. The means of five independent experiments are shown with SD. Fusion activity in the positive controls varied from 2.29 to 5.45 U. (B) LPC and Vam7p in vacuole fusion. Standard fusion reactions were supplemented with 420 μM LPC-12 and 300 nM of purified recombinant Vam7p (rVam7) as indicated and incubated on ice for 10 min. An ATP-regenerating system or buffer was added, and fusion was started by incubating samples at 27°C. After 70 min, fusion activity was determined. The means ± SD of four independent experiments is shown.

Results

LPCs inhibit in vitro fusion of yeast vacuoles

In vitro fusion of yeast vacuoles recapitulates the in vivo fusion of these organelles but provides accessibility to low and high molecular weight inhibitors. The reaction can be traced by a content-mixing assay relying on transfer of a lumenal vacuolar protease between the fusion partners. Vacuoles are prepared from two strains. One strain (BJ3505) expresses pro-alkaline phosphatase (ALP) in its vacuoles, and the other (DKY6281) expresses the respective maturation enzyme proteinase A. Upon fusion between the vacuoles, proteinase A from one vacuole can mature pro-ALP from the other fusion partner and activate it. The resulting enzymatic activity can be assayed by spectrophotometry. It serves as a quantitative readout of fusion.

We investigated the effects of LPC on vacuole fusion by titrating LPCs of different acyl chain lengths into fusion reactions. LPCs spontaneously incorporate into lipid bilayers. They lack the fatty acid at the sn-C2 position of the glycerol backbone, conferring an inverted cone shape. At the C1 position, different fatty acids can be attached via ester linkages. We tested 1-caprylyl, 1-capryl, 1-lauroyl, and 1-myristoyl LPCs, carrying saturated fatty acids with 8, 10, 12, or 14 carbon atoms, respectively. All LPCs inhibited the fusion of yeast vacuoles (Fig. 1 A). The IC_{50} values increased from 30 μM for LPC-14 (1-myristoyl-2-hydroxy-sn-glycero-3-phosphocholine) to 3 mM for LPC-8 (1-caprylyl-2-hydroxy-sn-glycero-3-phosphocholine), depending on the hydrocarbon chain length of the respective LPC. A similar trend was reported for influenza HA fusion (Chernomordik et al., 1997). This suggests that LPCs inhibit vacuole fusion and viral fusion by the same principle. Because the proteins involved in both reactions are very different, LPCs most likely inhibit via a structural influence on the lipid bilayer rather than a deleterious effect on a fusion protein.

Recently, Thorngren et al. (2004) found that addition of the recombinant t-SNARE subunit Vam7p (rVam7p) leads to the accumulation of excess trans-SNAREs and renders vacuole fusion independent of several early acting components, such as ATP and Sec18p/NSF-mediated priming. LPC suppressed rVam7p-mediated fusion (Fig. 1 B), suggesting that it acts on a late step of vacuolar membrane fusion.

LPCs block vacuole fusion after vacuole docking

The latest reaction phase blocked by an inhibitor can be inferred from the kinetics with which the reaction becomes insensitive to the inhibitor. In such an experiment, a fusion reaction is

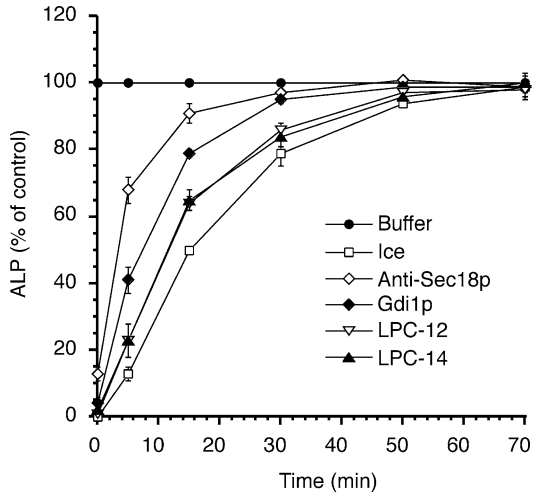

Figure 2. **Time course of inhibition by LPC.** 10× standard fusion reactions were started. 10 min before the indicated time points, 30-μl aliquots were supplemented with 1.5 μl of the indicated inhibitors or of buffer and placed on ice for 10 min. At the indicated time points, the samples were returned to 27°C and incubated until the end of the total reaction period of 70 min. One sample was kept on ice for each time point. The means of four independent experiments normalized to the controls are shown with SD. Fusion activity varied between 3.52 and 5.5 U. The following inhibitors were used: 0.3 μM anti-Sec18p antibody, 1 μM Gdi1p, 650 μM LPC-12, and 140 μM LPC-14.

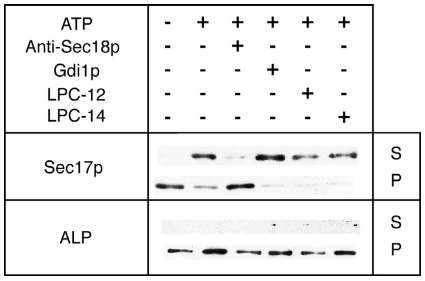

Figure 3. **Priming in the presence of LPC.** 3× standard fusion reactions without ATP-regenerating system were preincubated with the indicated inhibitors (5 min, 0°C). The ATP-regenerating system or control buffer was added, and reactions were started by incubation at 27°C. The sample without ATP was kept on ice. After 15 min, the reactions were stopped by chilling on ice. 1 ml PS buffer with 150 mM KCl was added, and vacuoles were sedimented (21,000 *g*, 3 min, 4°C). 900 μl of the supernatant was transferred to a new reaction tube, TCA precipitated, and analyzed by SDS-PAGE and Western blotting. Vacuole pellets were resuspended in 200 μl of fusion buffer with 150 mM KCl, transferred to a new reaction tube, and centrifuged (21,000 *g*, 3 min, 4°C). Pellets were analyzed by SDS-PAGE and Western blotting. The following inhibitors were used: 0.3 μM anti-Sec18p antibody, 1 μM Gdi1p, 500 μM LPC-12, and 120 μM LPC-14.

incubated at 27°C. At certain time points, aliquots are removed, supplemented either with buffer (control; no change in the final fusion activity should be observed) or with inhibitor, and incubated further at 27°C until the end of a standard 70-min reaction period. Progression of an uninhibited reaction is monitored by transferring one aliquot to 0°C at every time point. This stops the reaction. The ice curve is indicative of fusion pore opening because there is no significant delay between contents mixing and the processing of the reporter pro-ALP (Merz and Wickner, 2004a). The reaction became insensitive to antibody inhibition of the priming ATPase Sec18p/NSF within 15 min (Mayer et al., 1996; Fig. 2). Gdi1p (guanine nucleotide dissociation inhibitor), which binds and partially extracts the Rab-GTPase Ypt7p from the membrane (Mayer and Wickner, 1997) and thereby blocks docking, inhibited up to 30 min. Inhibitors blocking the reaction between docking and fusion pore opening, such as the chelator 1,2-bis-(o-aminophenoxy)-ethane-N,N,N′,N′-tetraacetic acid (BAPTA) and guanosine-5′-(γ-thio)triphosphate (GTPγS), yield inhibition curves between those of Gdi1p and ice (Mayer et al., 1996; Peters and Mayer, 1998; Peters et al., 1999; Reese et al., 2005). LPC-14 and -12 showed such inhibition kinetics. The time courses for both inhibitors overlapped, suggesting that they affect the same late step of the reaction and act by the same mechanism. Because LPCs inhibit other fusion systems at the lipid-mixing stage (Chernomordik et al., 1998; Melikyan et al., 2000), this result suggests that lipid mixing is kinetically distinguishable from docking and significantly precedes contents mixing.

The analysis in the preceding paragraph does not rule out the possibility that LPCs additionally inhibit earlier reaction steps. Therefore, we scored molecular marker events for priming and docking. Priming separates vacuolar cis-SNARE complexes through the action of Sec18p/NSF and Sec17p/α-SNAP (Ungermann et al., 1998a). As a consequence, Sec17p/α-SNAP is released from the vacuole into the supernatant (Mayer et al., 1996). We tested the influence of LPC-14 and -12 on Sec17p/α-SNAP release (Fig. 3). The vacuolar membrane protein ALP was blotted as a control for complete separation of membranes and supernatant. When vacuoles were incubated under fusion conditions without an ATP-regenerating system, Sec17p/α-SNAP remained associated with the vacuoles (Fig. 3). After addition of an ATP-regenerating system, Sec17p/ α-SNAP was released into the supernatant within 15 min. Antibodies to NSF/Sec18p inhibited this reaction, whereas the docking inhibitor Gdi1p did not influence it. Neither LPC-14 nor -12 blocked Sec17p release.

Docking results in the trans-association of v- and t-SNAREs from opposing membranes. The in vitro fusion reaction of yeast vacuoles offers the opportunity to assay this association and to determine whether trans-SNARE pairing correlates to fusion activity (Ungermann et al., 1998a,b; Merz and Wickner, 2004b). To this end, vacuoles are prepared from strains expressing only the vacuolar t-SNARE Vam3p or the v-SNARE Nyv1p. After mixing these two populations of vacuoles and incubating them in the presence of postdocking inhibitors of fusion, the membranes are diluted and solubilized. The trans-association of v- and t-SNAREs can then be assayed by coimmunoprecipitation of the v-SNARE Nyv1p with antibodies to the t-SNARE Vam3p. In the absence of a fusion inhibitor, these complexes represent a mixture of three species: trans-SNARE complexes between vacuoles that did not complete fusion; trans-SNARE complexes converted into cis-SNARE complexes because they triggered successful fusion of the vacuoles; and cis-SNARE complexes formed independently of docking by reassociation of solitary v- and t-SNAREs subsequent to the completion of fusion, i.e., as a simple result of membrane mixing between the v- and t-SNARE–carrying membranes. In the

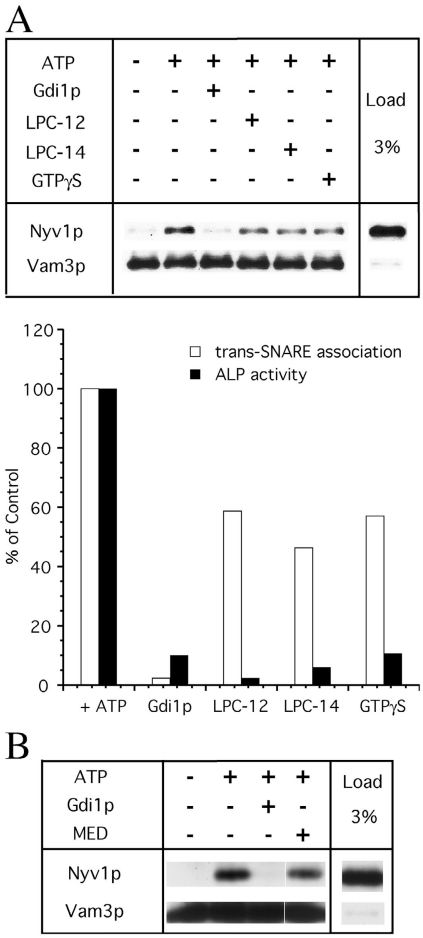

Figure 4. **Trans-SNARE complex formation.** Effects of LPC (A) and MED (B). 20× standard fusion reactions with vacuoles isolated from strains BJ3505 Δvam3 and BJ3505 Δnyv1 were started. Where indicated, the ATP-regenerating system was omitted and the sample was kept on ice. After 30 min, the reactions were stopped by chilling on ice. 380 μl of precipitation buffer was added (150 mM KCl, 1.3% [wt/vol] Triton X-100, 1.3 mM PMSF, 1.2× PIC, and 13 mM EDTA in PS). Samples were shaken for 10 min at 4°C and centrifuged at 21,000 *g* (10 min, 4°C). 450 μl of the solubilisate were transferred to a new reaction tube. 18 μg of affinity-purified anti-Vam3p antibody and 20 μl of protein A–Sepharose CL-4B (GE Healthcare) in 100 μl of washing buffer (150 mM KCl, 1% [wt/vol] Triton X-100, 1 mM PMSF, 1× PIC, and 10 mM EDTA in PS) were added to each sample. After 1 h of shaking at 4°C, the beads were washed with precipitation buffer and resuspended in SDS sample buffer. Aliquots were analyzed by SDS-PAGE and Western blotting. For A, trans-SNARE pairing was quantified by densitometry and compared with fusion activity that was determined from identical samples run in parallel (60 min, 27°C). The following inhibitors were used: 1 μM Gdi1p, 500 μM LPC-12, 120 μM LPC-14, 4 mM GTPγS, and 10 μM MED.

presence of late-acting fusion inhibitors, only the first species should accumulate. We tested for the formation of trans-SNARE complexes in the presence of LPCs. Without an ATP-regenerating system, priming and docking cannot occur and no Nyv1p could be coimmunoprecipitated with Vam3p (Fig. 4). In the presence of ATP, SNARE complexes formed. Simultaneous addition of the docking inhibitor Gdi1p completely blocked the formation of SNARE complexes, indicating that they resulted from docking. Similar to GTPγS, an established late-acting inhibitor of the postdocking phase, both LPC-14 and -12 allowed trans-SNARE pairing (Fig. 4), albeit only up to 50% of the uninhibited control. GTPγS permits docking as well as lipid mixing. Thus, the levels of trans-SNARE pairing reached in the presence of GTPγS should suffice to trigger lipid mixing. To assay the correlation between trans-SNARE pairing and fusion activity by independent means, we used another, recently identified inhibitor of vacuole fusion, myristoylated alanine-rich C kinase substrate effector domain peptide (MED; Fratti et al., 2004). MED sequesters phosphatidylinositol-4,5-bisphosphate, binds calmodulin with a K_d of 4 nM, and penetrates the acyl chain zone of lipid bilayers with its five phenylalanines (Sundaram et al., 2004). All three effects could contribute to its inhibitory activity in vacuole fusion. We observed that MED strongly promoted mutual binding and cluster formation of vacuoles (unpublished data). In accordance with this, MED permitted SNARE pairing to at least the same levels as in the uninhibited control, and in some experiments even twofold more (Fig. 4 B). Nevertheless, MED blocked content as well as lipid mixing (see next paragraph). Together, these results suggest that trans-SNARE complexes can efficiently form in the absence of lipid mixing. Furthermore, they show that LPCs and MED permit trans-SNARE association but interfere with vacuole fusion downstream of docking.

LPC inhibits lipid mixing in vacuolar membrane fusion

To determine whether LPC inhibited merging of the membranes or fusion pore formation, we used a novel assay for vacuolar membrane fusion that detects the fusion-dependent flow of lipids from one fusion partner to the other (Reese et al., 2005). This assay is based on the concentration-dependent change in fluorescence intensity of lissamine rhodamine B 1,2-dihexadecanoyl-sn-glycero-3-phosphoethanolamine (Rh-PE; rhodamine dye coupled to dipalmitoyl-phosphatidylethanolamine). We incorporated self-quenching concentrations (3 mole percent) of Rh-PE into the membranes of vacuoles isolated from one of our standard fusion strains (DKY6281) and mixed them with a sixfold excess of unlabeled vacuoles isolated from the other fusion strain (BJ3505). Upon fusion, the labeled phospholipids are diluted into the unlabeled BJ3505 membrane, which increases the relative fluorescence of rhodamine. Fusion reactions of identical composition can be tested for content mixing via the common vacuole fusion assay, which is based on the activation of pro-ALP in BJ3505 vacuoles by processing proteases provided by DKY6281 vacuoles. We titrated LPC-12 and MED into fusion reactions to test in parallel how LPC influences lipid and content mixing (Fig. 5). LPC-12 and MED inhibited both content- and lipid-mixing signals to comparable degrees. Thus, LPC and MED already suppress the lipid-mixing step of vacuolar membrane fusion.

LPC blocks formation of V_0 trans-complexes

V_0 sectors undergo a transformation in the final phase of vacuole fusion, which can be diagnosed by the association of V_0 sectors from opposing membranes (Peters et al., 2001; Bayer et al., 2003). V_0–V_0 association preferentially affects a population of

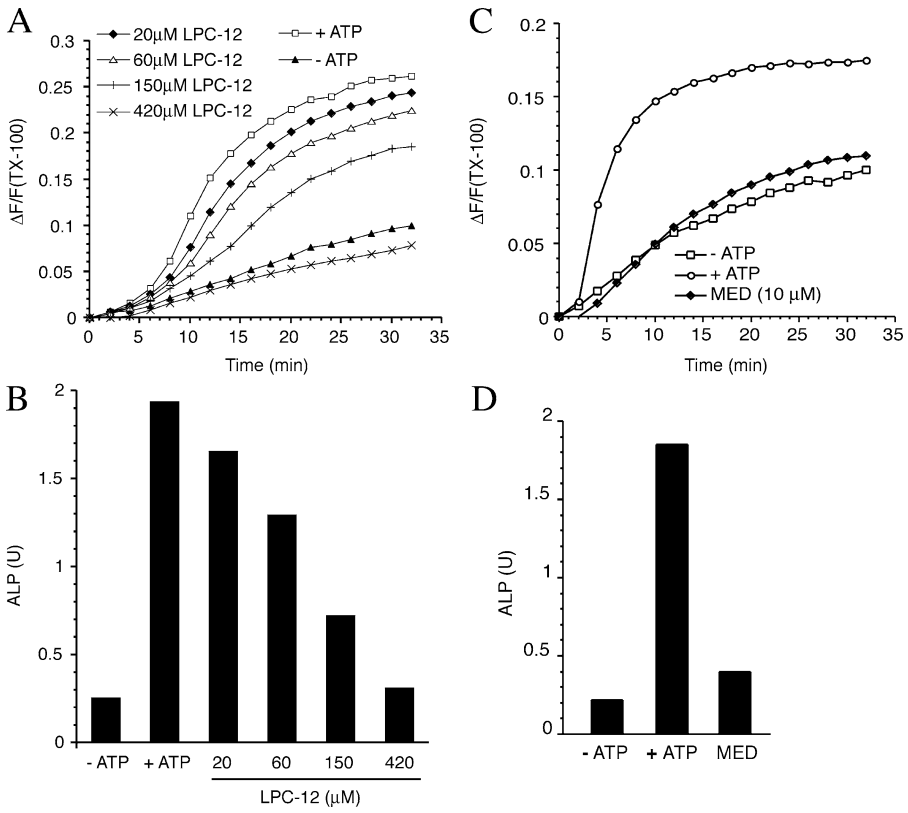

Figure 5. **Lipid mixing in the presence of LPC and MED.** (A and C) Fusion reactions with vacuoles containing rhodamine-labeled lipids were set up. After addition of unlabeled acceptor vacuoles, fusion-dependent dilution of the lipids was monitored via the increase in relative fluorescence. Reactions were run in the presence of control buffer or of LPC as indicated. (B and D) Content mixing was assayed from identical samples run in parallel.

V_0 sectors associated with the vacuolar t-SNARE Vam3p. It is a diagnostic criterion linked to the fusion cascade because it depends on vacuole priming and docking and is sensitive to the postdocking inhibitor BAPTA but insensitive to the latest acting inhibitor of vacuole fusion, GTPγS. Lipid transition mapped to the same stage as V_0 transformation, i.e., it was insensitive to GTPγS but sensitive to BAPTA (Reese et al., 2005). This suggests that V_0 transformation coincides with the induction of lipid flow. If so, changing lipid bilayer conformation by LPC might in turn influence V_0 transformation. We tested the formation of V_0 trans-complexes in the presence of LPCs or MED (Fig. 6). Vacuoles were prepared from two strains carrying either an HA or an AU tag on the V_0 subunit Vph1p. The membranes were incubated under fusion conditions in the presence of various inhibitors. They were then solubilized, and Vph1p-HA was precipitated with a monoclonal anti-HA antibody. Vph1p-AU that was coimmunoprecipitated with Vph1p-HA was detected by Western blotting against the AU tag. Without ATP, a condition preventing priming and docking, no Vph1p trans-association was detected (Fig. 6 A). With ATP, Vph1p-AU coimmunoprecipitated with Vph1p-HA, indicating a stable association of the proteins. Gdi1p, the docking inhibitor that prevents trans-SNARE pairing, suppressed the formation of these V_0–V_0 complexes as completely as MED. In contrast, GTPγS, which inhibits after lipid mixing, permitted formation of V_0 complexes, although it reduced fusion by >95%. In line with previous observations (Peters et al., 2001), this confirmed that the V_0–V_0 complexes observed arose from trans-association of V_0–V_0 sectors from two fusion partners before completion of fusion. LPC prevented V_0 trans-association (Fig. 6 A). We also checked whether LPC destabilized an existing trans-association of V_0. To this end, we ran fusion reactions for 40 min in the presence of GTPγS to generate V_0 trans-complexes. LPC was added and, after 10 min of further incubation, the vacuoles were solubilized and assayed for V_0 trans-complexes. The association of preformed V_0 trans-complexes was only slightly affected by subsequent addition of LPCs (Fig. 6 B), demonstrating that LPCs do not destabilize V_0 trans-complexes but interfere with their formation.

LPC arrests vacuole fusion at a productive intermediate state

Because LPCs reversibly incorporate into membranes, we tried to rescue the fusion block by removing LPCs again (Chernomordik et al., 1997; Melikyan et al., 2000). Fusion reactions were started in the presence of LPC. After 40 min, LPC was extracted from the membranes by floating the vacuoles through fatty acid–free bovine serum albumin. New fusion reactions were set up with these reisolated organelles and tested for their sensitivities toward inhibitors (Fig. 7). Good fusion activity was recovered after removing LPC. This shows that the vacuoles were not irreversibly damaged by LPC. Fusion after reversing the LPC block was insensitive to the docking inhibitor Gdi1p, as expected from the kinetic analysis (Fig. 2) and the docking assay (Fig. 4). The reaction stayed sensitive, however, to the postdocking inhibitors BAPTA and GTPγS. This indicates that the LPC block is reversible, that the intermediate accumulating in the presence of LPC is productive, and that the BAPTA- and GTPγS-sensitive steps cannot be passed before the LPC-sensitive stage.

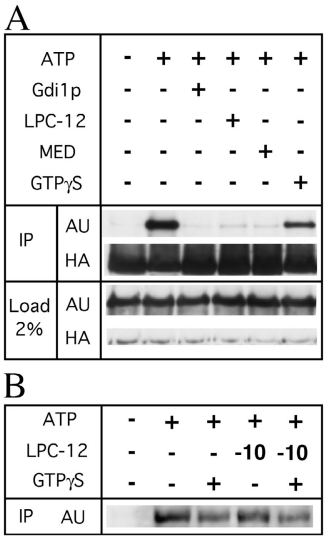

Figure 6. **V_0 trans-complexes in the presence of LPC.** (A) 15× standard fusion reactions with cytosol were started using vacuoles from strains BJ Vph1-HA and -AU and the indicated inhibitors. One sample did not contain an ATP-regenerating system and was kept on ice. After 50 min, the reactions were stopped by chilling on ice and adding 1 ml PS buffer. Vacuoles were pelleted by centrifugation (21,000 *g*, 2 min, 4°C). Pellets were solubilized in 1.3 ml of precipitation buffer (150 mM KCl, 0.5 mM $MnCl_2$, 1% [wt/vol] Triton X-100, and 1 mM PMSF in PS), shaken for 5 min at 4°C, and pelleted by centrifugation (21,000 *g*, 3 min, 4°C). To 1.1 ml of the solubilisate, 5 μl of monoclonal anti-HA antibody (raw ascites; 5–7 mg/ml) and 20 μl of protein G–Agarose was added. After 1 h of gentle shaking at 4°C, samples were washed with precipitation buffer, solubilized in SDS sample buffer, and analyzed by SDS-PAGE and Western blotting. (B) Stability of existing V_0 trans-complexes against LPC-12. Fusion reactions were run as in A but without LPC-12. 40 min after the start of fusion, two of the samples (−10) were supplemented with LPC-12 in order to test the effect of LPC addition on V_0 trans-complexes that had formed during the first 40 min. All samples were incubated for another 10 min at 27°C and then assayed for V_0 trans-complexes as in A. The following inhibitors were used: 1 μM Gdi1p, 500 μM LPC-12, 10 μM MED, and 4 mM GTPγS.

Fusion proceeds with similar rates from early and late intermediates

The availability of several reversible and late-acting inhibitors enabled us to compare the kinetics of vacuole fusion after release from these blocks. Should an early subreaction be rate limiting, a reaction arrested at a stage past this rate-limiting event should proceed significantly faster than a standard reaction. In contrast, if a late event in the reaction cascade is rate limiting, a reaction rescued from arrest before or at this rate-limiting step should run with a similar rate as an uninhibited reaction. We determined fusion kinetics after release from reversible blocks. Fusion was started in the presence of the inhibitors to allow the vacuoles to proceed up to the targeted reaction stage. Then the vacuoles were reisolated to remove the inhibitors and used in new fusion reactions. After restarting the reactions, aliquots were transferred to 0°C in 10-min intervals to stop further fusion and monitor the progress of the reaction. We compared the fusion rates after release from postdocking blocks with LPC, GTPγS, and BAPTA to those of reactions released from a high-salt block (250 mM KCl, which arrests fusion at docking; unpublished data) and to a reaction without inhibitor, in which fusion had been prevented by omission of ATP.

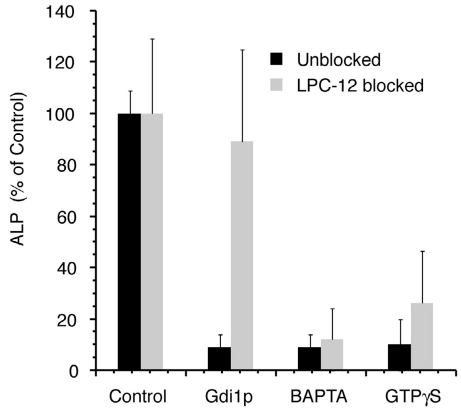

Figure 7. **The fusion block with LPC is reversible.** A 20× standard fusion reaction was started in the presence of 450 μM LPC-12. After 40 min at 27°C, 800 μl PS buffer with 15% (wt/vol) Ficoll and 0.5 mg/ml fatty acid–free bovine serum albumin were added. 300 μl PS buffer with 4% (wt/vol) Ficoll and 400 μl PS buffer were layered on top. Vacuoles were floated by centrifugation (21,000 *g*, 5 min, 4°C), recovered from the 0%/4% interface, and assayed for protein content. The recovered vacuoles were used in new standard fusion reactions with the indicated inhibitors. After 80 min, fusion was assayed. Control fusion reactions that had not been blocked with LPC and released were run in parallel. Their fusion activity was determined after 80 min at 27°C. Four independent experiments were averaged. Ice values had been subtracted. For the blocked and released reactions, ice values varied from 0.58 to 0.97 U and fusion activities varied from 2.2 to 4.2 U. For the unblocked reactions, ice values varied from 0.2 to 0.35 U and control values varied from 2.5 to 4.2 U. The following inhibitors were used: 1 μM Gdi1p, 5 mM BAPTA, and 4 mM GTPγS.

MED was not used in this experiment because its inhibitory effect was not reversible by a simple washing of the membranes (unpublished data). The rates after recovery from all reversible blocks were similar to that of an uninhibited standard reaction (Fig. 8). It appears unlikely that incomplete removal of the inhibitors after the block or slow dissociation of the inhibitors from their targets could limit the fusion rate after rescue because the inhibitors are unrelated by chemical structure and by mode of action. Therefore, the rate-limiting step of vacuole fusion should lie at or beyond the stages sensitive to LPC, BAPTA, and GTPγS. Because docking and lipid flow between the fusion partners occurs in the presence of GTPγS (Reese et al., 2005), our data suggests that the rate-limiting step in the fusion pathway lies downstream of these events.

In sum, our results provide a basis to kinetically map the requirement for lipid transition in the reaction sequence of vacuole fusion (Fig. 9). LPCs permit priming and docking. Lipid conformation is crucial for the transition from docking to fusion, i.e., to complete the BAPTA- and GTPγS-sensitive steps and to induce the conformational change of V_0, which occurs between docking and full fusion.

Discussion

Observations from this study can be integrated with previous data to define the order of events in the postdocking phase of vacuole fusion. LPC-blocked fusion reactions remain sensitive to the fast-acting Ca^{2+} chelator BAPTA and to GTPγS, suggesting that the LPC-sensitive step precedes events targeted by

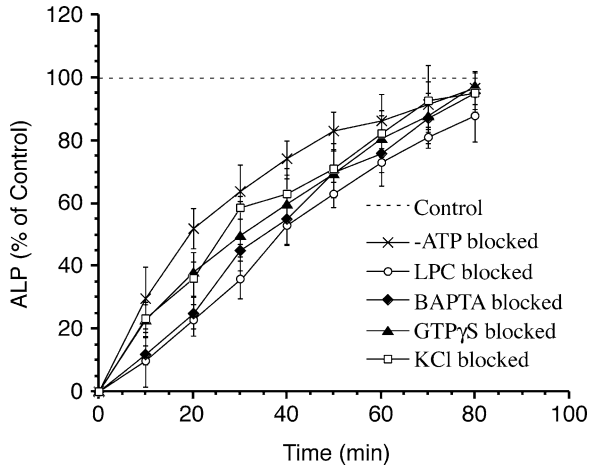

Figure 8. **Fusion kinetics after fusion block.** Vacuoles were preincubated under fusion conditions with 5 mM BAPTA, 4 mM GTPγS, 420 μM LPC-12, and 250 mM KCl or without ATP-regenerating system for 40 min. Vacuoles were then reisolated as in Fig. 7 and used to set up new fusion reactions without inhibitors. Aliquots were removed every 10 min and set on ice. After 80 min, fusion was assayed. Four independent experiments were averaged. Measured ALP activities varied from 0.4 to 0.6 U for the 0-min value and from 1.6 to 2.3 U for the 80-min value.

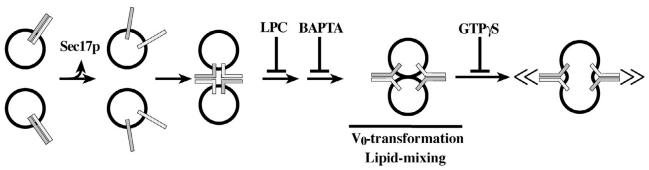

Figure 9. **Working model of late subreactions in vacuolar membrane fusion.** SNAREs are initially found in cis-complexes in the same membrane composed of v- and t-SNAREs (light and dark gray, respectively). They are disassembled by the action of NSF/Sec18p and its cofactor α-SNAP/Sec17p during priming. Upon priming, Sec17p is released as soluble protein. The action of several proteins leads to docking and the formation of trans-SNARE complexes. LPC acts before the BAPTA-sensitive step. A late subreaction involves conformational changes in the V_0 sector of the vacuolar ATPase, possibly resulting in lipid mixing. GTPγS inhibits fusion downstream of V_0 and lipid mixing.

these two inhibitors. In turn, BAPTA-blocked vacuoles become resistant to LPC. Trans-SNARE pairing is not prevented by any of these three inhibitors. These data suggest that trans-SNARE pairing is followed by an ordered sequence of steps defined by sensitivities to LPC, BAPTA, and GTPγS. Molecular events can now be grouped into this scheme: the transformation of V_0, which is diagnosed by their capacity to form V_0–V_0 trans-complexes; lipid transition by hemifusion; and fusion pore opening and contents mixing. LPC (Figs. 5 and 6) and BAPTA (Peters et al., 2001) block V_0 transformation and lipid transition between the fusion partners, whereas GTPγS permits these reactions and only blocks final opening of the fusion pore (Reese et al., 2005). Thus, V_0 transformation and lipid flow kinetically map to the same stage between BAPTA and GTPγS. Because LPC and, by inference, bilayer conformation and spontaneous curvature influence V_0 transformation, all kinetic and molecular observations link V_0 to the induction of lipid transition.

When released from blocks with postdocking inhibitors, vacuoles arrested by LPC, BAPTA, or GTPγS completed fusion with comparable kinetics as uninhibited reactions. This strongly suggests that reactions blocked with either of the three inhibitors still have to pass the rate-limiting step that seems to be the same for all of them and hence should lie past the latest acting of these inhibitors, GTPγS. Several studies demonstrate that the assay system is not rate limiting. The vacuolar content-mixing assay requires activation of the lumenal pro-ALP by two soluble proteases (Pep4p and Prb1p) from the other fusion partner. A detailed study on the kinetics of pro-ALP conversion by Pep4p and Prb1p (Merz and Wickner, 2004a) showed that this step is not rate limiting in the in vitro fusion assay. Also, in vivo mature ALP appears with a half time of 6 min (Klionsky and Emr, 1989), which includes transport through the biosynthetic pathway to the vacuole. Therefore, pro-ALP activation in vacuoles takes much less than 6 min, and the rate-limiting process must be inherent in the fusion cascade.

What could this rate-limiting step of fusion be? Theoretical considerations (Chizmadzhev et al., 2000; Cohen and Melikyan, 2004) and experimental observations on influenza HA–mediated fusion (Frolov et al., 2000; Markosyan et al., 2000) have suggested that opening and expansion of a fusion pore rather than induction of lipid transition may be the most energy demanding step of fusion. In line with this, our observations place the rate-limiting step past the GTPγS-sensitive intermediate, i.e., at the transition from lipid mixing to fusion pore opening (Reese et al., 2005). This suggests that fusion pore opening rather than trans-SNARE pairing or induction of lipid mixing is rate limiting for vacuole fusion. Our results hence provide experimental evidence from a physiological SNARE-dependent fusion system that is consistent with the theoretical predictions postulating that opening the pore may carry the highest cost of energy and be rate limiting. With our current methodology, we could not differentiate between substeps of fusion pore opening, e.g., the opening of initial small pores and their expansion. Our content-mixing assay requires transfer of an ∼40-kD protease and hence measures a relatively large pore. It may not allow for distinguishing very small initial pores, which could already be observed in other systems (Breckenridge and Almers, 1987; Zimmerberg et al., 1987, 1994; Curran et al., 1993; Lollike et al., 1995; Chanturiya et al., 1997; Lindau and Alvarez de Toledo, 2003), from the final, fully expanded state.

Because both SNAREs and viral fusion proteins form helical bundles, mechanistic parallels should be considered (Chernomordik et al., 1997, 1998; Melikyan et al., 2000). Type I viral fusion proteins fold back onto themselves and form α-helical bundles (Eckert and Kim, 2001; Park et al., 2003). Formation of fully stabilized helical bundles need not precede but can even follow lipid transition and the formation of a fusion pore (Melikyan et al., 2000; Borrego-Diaz et al., 2003; Markosyan et al., 2003). Complete helical bundle formation by viral fusion proteins hence does not correlate with lipid mixing. It may rather assist in opening the fusion pore or stabilize it after its formation. Lipid mixing is induced by the membrane-perturbing activity of viral fusion peptides (Cherno-

mordik and Kozlov, 2003; Tamm et al., 2003; Cohen and Melikyan, 2004). SNAREs could act in a similar fashion, i.e., the helical bundle might serve to pin the membranes together and assist in fusion pore opening once lipid transition has been triggered by membrane-disturbing compounds.

Several observations are compatible with a role of SNAREs in fusion pore formation. First, in artificial liposomes the outcome of fusion depends on the density of SNAREs reconstituted into their membranes (Lu et al., 2005; Xu et al., 2005). Completion of fusion requires higher SNARE densities and, by inference, higher densities of trans-SNARE complexes than the induction of lipid flow. Second, flipped SNAREs expressed on the surface of cells can also mediate slow fusion of such cells. If their transmembrane helices are replaced by glycosylphosphatidylinositol anchors so that they cannot span the entire bilayer, fusion pore opening is inefficient and hemifusion becomes the frequent end state (Giraudo et al., 2005). Also, truncation of the authentic transmembrane helix of SNAREs favors hemifusion (Xu et al., 2005). That SNAREs themselves might form part of the fusion pore was proposed based on the observation that substitutions in the transmembrane anchors of t-SNAREs change the electrophysiological properties of exocytic fusion pores measured in living cells (Han et al., 2004). This was taken as an indication that the transmembrane anchors of multiple SNAREs may form a barrel that constitutes the initial fusion pore and dissociates upon fusion pore expansion. However, biochemical evidence for the existence of a SNARE barrel is still missing. The effects observed are also consistent with other arrangements of SNAREs, and the substitutions might influence the interaction of SNAREs with other fusion-relevant proteins at exocytic sites, of which there are many (Hong, 2005).

In contrast to the observations made mainly in liposome systems with reconstituted SNAREs, which are consistent with a direct role of SNAREs in fusion pore opening, other observations on physiological membrane systems are less compatible with this view. Proteolytic removal of SNAREs on sea urchin cortical vesicles does not abolish fusion if contact is established by other means (Coorssen et al., 2003; Szule et al., 2003). Alternatively, trans-SNARE complexes in this system can also be disassembled by adding low concentrations of Ca^{2+}. This does not prevent subsequent fusion either (Tahara et al., 1998). Also, vacuolar trans-SNARE complexes were reported to become dispensable for completing fusion from the docked state (Ungermann et al., 1998b).

In the mechanochemical fusion model (Sollner, 2004), trans-SNARE complexes were proposed to induce lipid mixing by progressively zipping up from their membrane distal to their membrane-proximal parts. An alternative hypothesis is that they could already be fully zipped at the docking stage, mainly pinning the membranes together but requiring other factors to efficiently induce fusion. Several observations argue for the latter model. First, in this study we observed that reduction or enhancement of trans-SNARE pairing does not lead to comparable reduction or enhancement of lipid mixing. Second, during trans-SNARE complex formation in proteoliposomes, the entire SNARE domains can pair in a single step, but fusion follows complete core-complex formation with a long lag time (Zhang et al., 2004). Third, in case of progressive helix zippering toward the membrane anchors, one might expect competitive inhibition by peptides corresponding to the membrane-proximal COOH-terminal part of the v-SNARE. This was not observed (Melia et al., 2002), although analogous viral peptides could block formation of the helical bundle (Eckert and Kim, 2001). Finally, additional proteins are required for the transition from trans-SNARE pairing to lipid mixing or complete vacuole fusion, such as Vac8p (Wang et al., 2001) and V_0 (Peters et al., 2001; Bayer et al., 2003). Also, fusion of docked secretory vesicles in *Drosophila melanogaster* requires V_0, as demonstrated recently (Hiesinger et al., 2005).

LPC and the positive curvature of the membrane affect a step past membrane docking and block subsequent transformation of V_0 and lipid mixing. Therefore, we propose that docking and lipid mixing are separable events in SNARE-dependent fusion reactions. Trans-SNAREs may hold the membranes in close proximity and possibly modify downstream factors, in particular V_0, which are required to trigger fusion. Such an interpretation is consistent with the picture from viral fusion where membrane apposition and fusion pore opening via helical bundles are separable from the induction of lipid mixing via the fusion peptide (Qiao et al., 1999; Melikyan et al., 2000). In both systems, the last step, opening the fusion pore, appears to be the most demanding and rate-limiting event.

Materials and methods

LPC-8, LPC-10 (1-capryl-2-hydroxy-sn-glycero-3-phosphocholine), LPC-12 (1-lauroyl-2-hydroxy-sn-glycero-3-phosphocholine), and LPC-14 were purchased from Avanti Polar Lipids, Inc. 20 mM of stock solutions of the LPCs in PS buffer (200 mM sorbitol and 10 mM Pipes/KOH, pH 6.8) were stored at −20°C. Rh-PE was obtained from Invitrogen. Fatty acid–free bovine serum albumin and analytical grade dimethyl sulfoxide were obtained from Sigma-Aldrich. 3 mM Rh-PE stock solutions in DMSO were stored at −20°C. Production and purification of polyclonal antibodies to Sec18p, Sec17p, Vam3p, and Nyv1p were described previously (Haas and Wickner, 1996; Mayer et al., 1996; Nichols et al., 1997). Anti-HA monoclonal mouse antibodies (raw ascites) and monoclonal mouse AU antibodies were purchased from BaBCo. Monoclonal mouse antibody to ALP was purchased from Invitrogen. Gdi1p was recombinantly expressed and purified from *Escherichia coli* (Haas et al., 1995). GTPγS was obtained from Roche Molecular Biochemicals, and BAPTA was obtained from Calbiochem. PS buffer was used as a basis for most solutions. MED was produced by solid phase peptide synthesis and purified by HPLC.

Strains

BJ3505 and DKY6281 were the standard fusion strains. For the assay of trans-SNARE pairing, we used deletion strains for Vam3p and Nyv1p in BJ3505 (Nichols et al., 1997; Ungermann et al., 1998b). V_0 trans-complex formation was assayed with BJ3505 strains carrying either an AU (SBY129) or an HA tag (SBY119) on Vph1p (Peters et al., 2001).

Vacuole isolation and fusion

Yeast was precultured in yeast extract/peptone/dextrose (YPD) medium (6–8 h, 30°C). Overnight cultures were inoculated (30°C, 14–16 h; 225 rpm) in baffled 2-liter Erlenmeyer flasks with 1 liter of YPD medium. At an OD_{600} of 2–5, cells were centrifuged (5 min, 4,000 *g*, 23°C; JA10 rotor), resuspended in 50 ml of 0.1 M Tris/Cl, pH 8.9, with 10 mM DTT, incubated (10 min, 30°C), centrifuged (5 min, 4,000 *g*, 2°C; JA10 rotor), resuspended in 15 ml SB (50 mM potassium phosphate, pH 7.5, and 600 mM sorbitol in YPD with 0.2% dextrose and 3,600 U/ml oxalyticase for BJ3505 and 1,800 U/ml for DKY6281), and transferred into 30-ml Corex tubes. Cells were incubated (20 min, 30°C), reisolated (1 min, 800 *g*, then 1 min, 1,500 *g*, 2°C; JA20 rotor), and resuspended in 2.5 ml of

15% Ficoll 400 in PS buffer by gentle stirring with a glass rod. DEAE-dextran (200 μl for BJ3505 or 100 μl for DKY6281) was added from 0.4 mg/ml of a fresh stock in 15% Ficoll in PS buffer. The cells were incubated (2 min at 0°C and 75 s at 30°C), chilled again, transferred to a SW41 tube, and overlaid with 3 ml of 8% Ficoll, 3 ml of 4% Ficoll, and 1.5 ml of 0% Ficoll (all in PS buffer). After centrifugation (90 min, 150,000 *g*), the vacuoles were harvested from the 0%/4% interphase. The amount of the harvested 4% phase was minimized because it interferes with reisolation of the vacuoles in subsequent experiments. A standard fusion reaction contained 4 μg of vacuoles, isolated from strains BJ3505 and DKY6281, in a total volume of 31.5 μl of reaction buffer (20 mM Pipes/KOH, pH 6.8, 200 mM sorbitol, 125 mM KCl, 0.5 mM $MgCl_2$, 0.5 mM $MnCl_2$, 0.5 mM ATP, 7.5 μM pefablock SC, 7.5 ng/ml leupeptin, 3.75 μM *o*-phenanthroline, 37.5 ng/ml pepstatin A, 20 mM creatine phosphate, and 35 U/ml creatine kinase). The ATP-regenerating system, containing $MgCl_2$, ATP, creatine phosphate, and creatine kinase, was added from a frozen 20× stock solution in PS buffer with 150 mM KCl. After 60 min at 27°C, fusion was assayed.

Content-mixing assay

Content mixing was determined via ALP activity. Mature ALP is generated by transfer of proteinase A (contained in DKY6281 vacuoles) into BJ3505 vacuoles (carrying pro-ALP). After completion of the fusion reaction, vacuoles were lysed with 500 μl of a mixture containing 1 mM *p*-nitrophenylphosphate, 10 mM $MgCl_2$, 0.5% (wt/vol) Triton X-100, and 250 mM Tris/Cl, pH 8.9. After 4 min, 500 μl of 1 M glycine, pH 11.5, was added and the OD was read at 400 nm. 1 U of fusion activity is defined as 1 μmol/l *p*-nitrophenol developed per minute and microgram of BJ3505 vacuoles at 27°C. Ice values were subtracted.

Lipid-mixing assay

For the incorporation of Rh-PE into vacuolar membranes, 560 μg of freshly prepared vacuoles from strain DKY6281 were equilibrated in 800 μl PS buffer to 27°C for 1.5 min, 60 μl of 3 mM Rh-PE in DMSO were added under mild vortexing, and vacuoles were reisolated. 500 μl PS buffer containing 15% (wt/vol) Ficoll were added and mixed. On top, 300 μl PS buffer containing 4% and 400 μl PS buffer containing no Ficoll were layered. After centrifugation (5 min, 4°C, 11,500 *g*), the labeled vacuoles were recovered from the 4%/0% interface. 3× standard fusion reactions contained a sixfold excess of unlabeled vacuoles from strain BJ3505 over Rh-PE–labeled vacuoles isolated from strain DKY6281. For fluorescence measurements, the reactions were transferred into black noncoated microtiterplates (Nunc). Rhodamine fluorescence was measured with a fluorescent plate reader (SpectraMax GeminiXS; Molecular Devices) at 538 nm excitation and 585 nm emission. After completion of the reaction, the membranes were solubilized by adding 100 μl of 1% (wt/vol) Triton X-100 in PS buffer. Fluorescence was followed for another 10 min with the same settings as before, taking measurements every 30 s. The calculated average of the measurement after addition of Triton X-100 served as the fluorescence after infinite dilution (F(TX-100)). After addition of Triton X-100, we measured ~8,000 relative fluorescence units for all samples. For the 0-min values, we measured ~900 relative fluorescence units for all samples. Measured fluorescence of a sample before solublization was normalized to the fluorescence after infinite dilution, resulting in ΔF/F(TX-100) values. The resulting value for the 0-min time point was set to 0. Content mixing was measured in parallel samples via the established assay of ALP activity. To this end, 31.5-μl aliquots with an identical composition to the ones measured in the fluorescent plate reader were incubated at 27°C for 70 min.

We thank Monique Reinhardt, Andrea Schmidt, and Véronique Comte for assistance and Catherine Servis for synthesis of MED.

This work was supported by grants from the Deutsche Forschungsgemeinschaft, Fonds National Suisse, Human Frontier Science Program, and Boehringer Ingelheim.

Submitted: 5 October 2005
Accepted: 17 November 2005

References

Ahn, A., D.L. Gibbons, and M. Kielian. 2002. The fusion peptide of Semliki Forest virus associates with sterol-rich membrane domains. *J. Virol.* 76:3267–3275.

Bayer, M.J., C. Reese, S. Buhler, C. Peters, and A. Mayer. 2003. Vacuole membrane fusion: V_0 functions after trans-SNARE pairing and is coupled to the Ca^{2+}-releasing channel. *J. Cell Biol.* 162:211–222.

Borrego-Diaz, E., M.E. Peeples, R.M. Markosyan, G.B. Melikyan, and F.S. Cohen. 2003. Completion of trimeric hairpin formation of influenza virus hemagglutinin promotes fusion pore opening and enlargement. *Virology.* 316:234–244.

Breckenridge, L.J., and W. Almers. 1987. Currents through the fusion pore that forms during exocytosis of a secretory vesicle. *Nature.* 328:814–817.

Chanturiya, A., L.V. Chernomordik, and J. Zimmerberg. 1997. Flickering fusion pores comparable with initial exocytotic pores occur in protein-free phospholipid bilayers. *Proc. Natl. Acad. Sci. USA.* 94:14423–14428.

Chernomordik, L.V., and J. Zimmerberg. 1995. Bending membranes to the task: structural intermediates in bilayer fusion. *Curr. Opin. Struct. Biol.* 5:541–547.

Chernomordik, L.V., and M.M. Kozlov. 2003. Protein-lipid interplay in fusion and fission of biological membranes. *Annu. Rev. Biochem.* 72:175–207.

Chernomordik, L.V., S.S. Vogel, A. Sokoloff, H.O. Onaran, E.A. Leikina, and J. Zimmerberg. 1993. Lysolipids reversibly inhibit Ca(2+)-, GTP- and pH-dependent fusion of biological membranes. *FEBS Lett.* 318:71–76.

Chernomordik, L., A. Chanturiya, J. Green, and J. Zimmerberg. 1995. The hemifusion intermediate and its conversion to complete fusion: regulation by membrane composition. *Biophys. J.* 69:922–929.

Chernomordik, L.V., E. Leikina, V. Frolov, P. Bronk, and J. Zimmerberg. 1997. An early stage of membrane fusion mediated by the low pH conformation of influenza hemagglutinin depends upon membrane lipids. *J. Cell Biol.* 136:81–93.

Chernomordik, L.V., V.A. Frolov, E. Leikina, P. Bronk, and J. Zimmerberg. 1998. The pathway of membrane fusion catalyzed by influenza hemagglutinin: restriction of lipids, hemifusion, and lipidic fusion pore formation. *J. Cell Biol.* 140:1369–1382.

Chizmadzhev, Y.A., P.I. Kuzmin, D.A. Kumenko, J. Zimmerberg, and F.S. Cohen. 2000. Dynamics of fusion pores connecting membranes of different tensions. *Biophys. J.* 78:2241–2256.

Cohen, F.S., and G.B. Melikyan. 2004. The energetics of membrane fusion from binding, through hemifusion, pore formation, and pore enlargement. *J. Membr. Biol.* 199:1–14.

Coorssen, J.R., P.S. Blank, F. Albertorio, L. Bezrukov, I. Kolosova, X. Chen, P.S. Backlund Jr., and J. Zimmerberg. 2003. Regulated secretion: SNARE density, vesicle fusion and calcium dependence. *J. Cell Sci.* 116:2087–2097.

Curran, M.J., F.S. Cohen, D.E. Chandler, P.J. Munson, and J. Zimmerberg. 1993. Exocytotic fusion pores exhibit semi-stable states. *J. Membr. Biol.* 133:61–75.

Eckert, D.M., and P.S. Kim. 2001. Mechanisms of viral membrane fusion and its inhibition. *Annu. Rev. Biochem.* 70:777–810.

Fratti, R.A., Y. Jun, A.J. Merz, N. Margolis, and W. Wickner. 2004. Interdependent assembly of specific regulatory lipids and membrane fusion proteins into the vertex ring domain of docked vacuoles. *J. Cell Biol.* 167:1087–1098.

Frolov, V.A., M.S. Cho, P. Bronk, T.S. Reese, and J. Zimmerberg. 2000. Multiple local contact sites are induced by GPI-linked influenza hemagglutinin during hemifusion and flickering pore formation. *Traffic.* 1:622–630.

Fuller, N., and R.P. Rand. 2001. The influence of lysolipids on the spontaneous curvature and bending elasticity of phospholipid membranes. *Biophys. J.* 81:243–254.

Giraudo, C.G., C. Hu, D. You, A.M. Slovic, E.V. Mosharov, D. Sulzer, T.J. Melia, and J.E. Rothman. 2005. SNAREs can promote complete fusion and hemifusion as alternative outcomes. *J. Cell Biol.* 170:249–260.

Haas, A., and W. Wickner. 1996. Homotypic vacuole fusion requires Sec17p (yeast alpha-SNAP) and Sec18p (yeast NSF). *EMBO J.* 15:3296–3305.

Haas, A., D. Scheglmann, T. Lazar, D. Gallwitz, and W. Wickner. 1995. The GTPase Ypt7p of *Saccharomyces cerevisiae* is required on both partner vacuoles for the homotypic fusion step of vacuole inheritance. *EMBO J.* 14:5258–5270.

Han, X., C.T. Wang, J. Bai, E.R. Chapman, and M.B. Jackson. 2004. Transmembrane segments of syntaxin line the fusion pore of Ca^{2+}-triggered exocytosis. *Science.* 304:289–292.

Hiesinger, P.R., A. Fayyazuddin, S.Q. Mehta, T. Rosenmund, K.L. Schulze, R.G. Zhai, P. Verstreken, Y. Cao, Y. Zhou, J. Kunz, and H.J. Bellen. 2005. The v-ATPase V_0 subunit a1 is required for a late step in synaptic vesicle exocytosis in *Drosophila*. *Cell.* 121:607–620.

Hong, W. 2005. SNAREs and traffic. *Biochim. Biophys. Acta.* 1744:493–517.

Kemble, G.W., T. Danieli, and J.M. White. 1994. Lipid-anchored influenza hemagglutinin promotes hemifusion, not complete fusion. *Cell.* 76:383–391.

Klionsky, D.J., and S.D. Emr. 1989. Membrane protein sorting: biosynthesis, transport and processing of yeast vacuolar alkaline phosphatase. *EMBO J.*

8:2241–2250.

Kozlovsky, Y., L.V. Chernomordik, and M.M. Kozlov. 2002. Lipid intermediates in membrane fusion: formation, structure, and decay of hemifusion diaphragm. *Biophys. J.* 83:2634–2651.

Lee, J., and B.R. Lentz. 1997. Evolution of lipidic structures during model membrane fusion and the relation of this process to cell membrane fusion. *Biochemistry.* 36:6251–6259.

Lindau, M., and G. Alvarez de Toledo. 2003. The fusion pore. *Biochim. Biophys. Acta.* 1641:167–173.

Lollike, K., N. Borregaard, and M. Lindau. 1995. The exocytotic fusion pore of small granules has a conductance similar to an ion channel. *J. Cell Biol.* 129:99–104.

Lu, X., F. Zhang, J.A. McNew, and Y.K. Shin. 2005. Membrane fusion induced by neuronal SNAREs transits through hemifusion. *J. Biol. Chem.* 280:30538–30541.

Markosyan, R.M., F.S. Cohen, and G.B. Melikyan. 2000. The lipid-anchored ectodomain of influenza virus hemagglutinin (GPI-HA) is capable of inducing nonenlarging fusion pores. *Mol. Biol. Cell.* 11:1143–1152.

Markosyan, R.M., F.S. Cohen, and G.B. Melikyan. 2003. HIV-1 envelope proteins complete their folding into six-helix bundles immediately after fusion pore formation. *Mol. Biol. Cell.* 14:926–938.

Mayer, A. 2002. Membrane fusion in eukaryotic cells. *Annu. Rev. Cell Dev. Biol.* 18:289–314.

Mayer, A., and W. Wickner. 1997. Docking of yeast vacuoles is catalyzed by the Ras-like GTPase Ypt7p after symmetric priming by Sec18p (NSF). *J. Cell Biol.* 136:307–317.

Mayer, A., W. Wickner, and A. Haas. 1996. Sec18p (NSF)-driven release of Sec17p (alpha-SNAP) can precede docking and fusion of yeast vacuoles. *Cell.* 85:83–94.

Meers, P., S. Ali, R. Erukulla, and A.S. Janoff. 2000. Novel inner monolayer fusion assays reveal differential monolayer mixing associated with cation-dependent membrane fusion. *Biochim. Biophys. Acta.* 1467:227–243.

Melia, T.J., T. Weber, J.A. McNew, L.E. Fisher, R.J. Johnston, F. Parlati, L.K. Mahal, T.H. Sollner, and J.E. Rothman. 2002. Regulation of membrane fusion by the membrane-proximal coil of the t-SNARE during zippering of SNAREpins. *J Cell Biol*. 158:929–940.

Melikyan, G.B., J.M. White, and F.S. Cohen. 1995. GPI-anchored influenza hemagglutinin induces hemifusion to both red blood cell and planar bilayer membranes. *J. Cell Biol.* 131:679–691.

Melikyan, G.B., R.M. Markosyan, H. Hemmati, M.K. Delmedico, D.M. Lambert, and F.S. Cohen. 2000. Evidence that the transition of HIV-1 gp41 into a six-helix bundle, not the bundle configuration, induces membrane fusion. *J. Cell Biol.* 151:413–423.

Melikyan, G.B., R.J. Barnard, L.G. Abrahamyan, W. Mothes, and J.A. Young. 2005. Imaging individual retroviral fusion events: from hemifusion to pore formation and growth. *Proc. Natl. Acad. Sci. USA.* 102:8728–8733.

Merz, A.J., and W.T. Wickner. 2004a. Resolution of organelle docking and fusion kinetics in a cell-free assay. *Proc. Natl. Acad. Sci. USA*. 101:11548–11553.

Merz, A.J., and W.T. Wickner. 2004b. Trans-SNARE interactions elicit Ca^{2+} efflux from the yeast vacuole lumen. *J. Cell Biol.* 164:195–206.

Munoz-Barroso, I., S. Durell, K. Sakaguchi, E. Appella, and R. Blumenthal. 1998. Dilation of the human immunodeficiency virus–1 envelope glycoprotein fusion pore revealed by the inhibitory action of a synthetic peptide from gp41. *J. Cell Biol.* 140:315–323.

Nichols, B.J., C. Ungermann, H.R. Pelham, W.T. Wickner, and A. Haas. 1997. Homotypic vacuolar fusion mediated by t- and v-SNAREs. *Nature.* 387:199–202.

Park, H.E., J.A. Gruenke, and J.M. White. 2003. Leash in the groove mechanism of membrane fusion. *Nat Struct Biol.* 10:1048–1053.

Pecheur, E.I., I. Martin, O. Maier, U. Bakowsky, J.M. Ruysschaert, and D. Hoekstra. 2002. Phospholipid species act as modulators in p97/p47-mediated fusion of Golgi membranes. *Biochemistry.* 41:9813–9823.

Peters, C., and A. Mayer. 1998. Ca^{2+}/calmodulin signals the completion of docking and triggers a late step of vacuole fusion. *Nature.* 396:575–580.

Peters, C., P.D. Andrews, M.J. Stark, S. Cesaro-Tadic, A. Glatz, A. Podtelejnikov, M. Mann, and A. Mayer. 1999. Control of the terminal step of intracellular membrane fusion by protein phosphatase 1. *Science.* 285:1084–1087.

Peters, C., M.J. Bayer, S. Buhler, J.S. Andersen, M. Mann, and A. Mayer. 2001. Trans-complex formation by proteolipid channels in the terminal phase of membrane fusion. *Nature.* 409:581–588.

Qiao, H., R.T. Armstrong, G.B. Melikyan, F.S. Cohen, and J.M. White. 1999. A specific point mutant at position 1 of the influenza hemagglutinin fusion peptide displays a hemifusion phenotype. *Mol. Biol. Cell.* 10:2759–2769.

Reese, C., F. Heise, and A. Mayer. 2005. Trans-SNARE pairing can precede a hemifusion intermediate in intracellular membrane fusion. *Nature.* 436:410–414.

Simonsen, A., A.E. Wurmser, S.D. Emr, and H. Stenmark. 2001. The role of phosphoinositides in membrane transport. *Curr. Opin. Cell Biol.* 13:485–492.

Sollner, T.H. 2004. Intracellular and viral membrane fusion: a uniting mechanism. *Curr. Opin. Cell Biol.* 16:429–435.

Sundaram, M., H.W. Cook, and D.M. Byers. 2004. The MARCKS family of phospholipid binding proteins: regulation of phospholipase D and other cellular components. *Biochem. Cell Biol.* 82:191–200.

Szule, J.A., S.E. Jarvis, J.E. Hibbert, J.D. Spafford, J.E. Braun, G.W. Zamponi, G.M. Wessel, and J.R. Coorssen. 2003. Calcium-triggered membrane fusion proceeds independently of specific presynaptic proteins. *J Biol. Chem*. 278:24251–24254.

Tahara, M., J.R. Coorssen, K. Timmers, P.S. Blank, T. Whalley, R. Scheller, and J. Zimmerberg. 1998. Calcium can disrupt the SNARE protein complex on sea urchin egg secretory vesicles without irreversibly blocking fusion. *J. Biol. Chem.* 273:33667–33673.

Tamm, L.K., J. Crane, and V. Kiessling. 2003. Membrane fusion: a structural perspective on the interplay of lipids and proteins. *Curr. Opin. Struct. Biol.* 13:453–466.

Thorngren, N., K.M. Collins, R.A. Fratti, W. Wickner, and A.J. Merz. 2004. A soluble SNARE drives rapid docking, bypassing ATP and Sec17/18p for vacuole fusion. *EMBO J*. 23:2765–2776.

Ungermann, C., B.J. Nichols, H.R. Pelham, and W. Wickner. 1998a. A vacuolar v–t-SNARE complex, the predominant form in vivo and on isolated vacuoles, is disassembled and activated for docking and fusion. *J. Cell Biol.* 140:61–69.

Ungermann, C., K. Sato, and W. Wickner. 1998b. Defining the functions of trans-SNARE pairs. *Nature.* 396:543–548.

Vogel, S.S., E.A. Leikina, and L.V. Chernomordik. 1993. Lysophosphatidylcholine reversibly arrests exocytosis and viral fusion at a stage between triggering and membrane merger. *J. Biol. Chem.* 268:25764–25768.

Wang, Y.X., E.J. Kauffman, J.E. Duex, and L.S. Weisman. 2001. Fusion of docked membranes requires the armadillo repeat protein Vac8p. *J. Biol. Chem.* 276:35133–35140.

Wickner, W. 2002. Yeast vacuoles and membrane fusion pathways. *EMBO J.* 21:1241–1247.

Wu, H., L. Zheng, and B.R. Lentz. 1996. A slight asymmetry in the transbilayer distribution of lysophosphatidylcholine alters the surface properties and poly(ethylene glycol)-mediated fusion of dipalmitoylphosphatidylcholine large unilamellar vesicles. *Biochemistry.* 35:12602–12611.

Xu, Y., F. Zhang, Z. Su, J.A. McNew, and Y.K. Shin. 2005. Hemifusion in SNARE-mediated membrane fusion. *Nat. Struct. Mol. Biol.* 12:417–422.

Zhang, F., Y. Chen, Z. Su, and Y.K. Shin. 2004. SNARE assembly and membrane fusion, a kinetic analysis. *J Biol. Chem*. 279:38668–38672.

Zimmerberg, J., M. Curran, F.S. Cohen, and M. Brodwick. 1987. Simultaneous electrical and optical measurements show that membrane fusion precedes secretory granule swelling during exocytosis of beige mouse mast cells. *Proc. Natl. Acad. Sci. USA.* 84:1585–1589.

Zimmerberg, J., R. Blumenthal, D.P. Sarkar, M. Curran, and S.J. Morris. 1994. Restricted movement of lipid and aqueous dyes through pores formed by influenza hemagglutinin during cell fusion. *J. Cell Biol.* 127:1885–1894.